IEEE Photonics Journal
An IEEE Photonics Society Publication

Open Access

Visible Light Positioning and Lighting Based on Identity Positioning and RF Carrier Allocation Technique Using a Solar Cell Receiver

Volume 8, Number 4, August 2016

Chin-Wei Hsu
Jhao-Ting Wu
Hao-Yu Wang
Chi-Wai Chow
Chun-Hsing Lee
Mu-Tao Chu
Chien-Hung Yeh

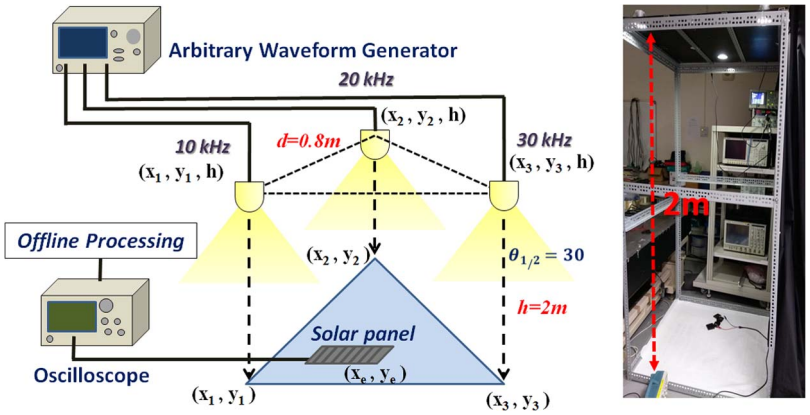

DOI: 10.1109/JPHOT.2016.2590945
1943-0655 © 2016 IEEE

IEEE photonics SOCIETY

IEEE

Visible Light Positioning and Lighting Based on Identity Positioning and RF Carrier Allocation Technique Using a Solar Cell Receiver

Chin-Wei Hsu,[1] Jhao-Ting Wu,[1] Hao-Yu Wang,[1] Chi-Wai Chow,[1] Chun-Hsing Lee,[2] Mu-Tao Chu,[2] and Chien-Hung Yeh[3]

[1]Department of Photonics and Institute of Electro-Optical Engineering, National Chiao Tung University, Hsinchu 300, Taiwan
[2]Industrial Technology Research Institute, Hsinchu 310, Taiwan
[3]Department of Photonics, Feng Chia University, Taichung 407, Taiwan

DOI: 10.1109/JPHOT.2016.2590945

Manuscript received May 18, 2016; revised June 14, 2016; accepted July 4, 2016. Date of publication July 13, 2016; date of current version July 28, 2016. This work was supported by the Ministry of Science and Technology, Taiwan, under Grant MOST-104-2628-E-009-011-MY3 and Grant MOST-103-2218-E-035-011-MY3; by The Aim for the Top University Plan; and by the Academic-Industrial Research Project of the Industrial Technology Research Institute, Taiwan. Corresponding author: C. W. Chow (e-mail: cwchow@faculty.nctu.edu.tw).

Abstract: We propose and experimentally demonstrate an indoor positioning system which combines identity positioning and the radio frequency carrier allocation technique in order to reduce the signal interference from nearby light-emitting diodes (LEDs) and improve the accuracy of positioning. In addition, the solar cell is used as an optical receiver for the visible light positioning system. Due to the benefits of solar cells such as low-cost, high light sensitivity, and ease in integration with wearable devices, the proposed system could be an energy-efficient and environmentally friendly choice for indoor positioning in the future.

Index Terms: Free-space communication, optical communications, light-emitting diodes (LEDs).

1. Introduction

In recent years, light-emitting diodes (LEDs) havb been widely used. They are replacing incandescent light bulbs and fluorescent lamps because LEDs conserve energy and provide extended lifetime compared to traditional lighting sources. Besides illumination, LED lighting can carry information, which is known as visible light communication (VLC) [1]. VLC can provide high security and directional communication link [2]–[5]. Besides, owing to the shortage of the radio-frequency (RF) spectrum, VLC is also regarded as one of the solutions for future fifth-generation (5G) wireless communications [6]. In addition to communication function, LED lighting can also be used for high accuracy positioning. The Global Positioning System (GPS) is now very popular; however, it does not work well inside buildings. One indoor positioning system utilizes identity positioning in which the receiver (Rx) detects the identity (ID) of the nearest LED transmitter (Tx) and then transmits this information to the central office using a radio system such as ZigBee or wireless local area network (WLAN) [7]. However, the positioning resolution of

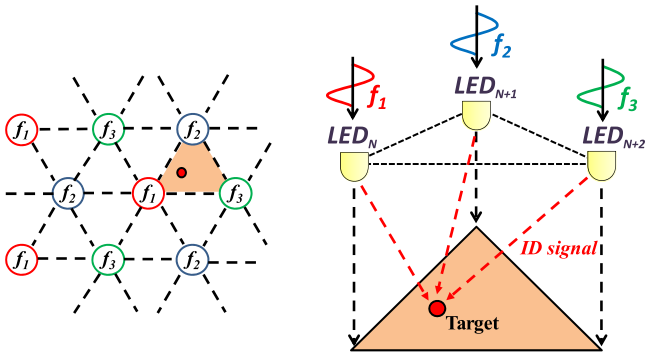

Fig. 1. Proposed architecture of visible light positioning system.

this system is low and cannot accurately perform positioning within the shined area of the LED lamp. In [8], an asynchronous indoor positioning system based on VLC is proposed; however, no experimental results are provided. In [9], a 3-D positioning system is reported; however the Rx orientation is required. Rx powers from each LED lamp should be measured twice by varying the Rx orientations; and accelerometer in the Rx is required. Hence, the system cost and complexity will be increased if smart-phone is not used as the positioning Rx. In [10], a multiple-input multiple-output (MIMO) VLC positioning system is demonstrated; however, two or more Rxs are needed for MIMO demodulation.

In this work, we utilize a trilateration positioning method which uses the received signal power to determine the distances between the Rx to each LED Tx, and can estimate the position of Rx with much higher accuracy in a small area. Then, we combine the identity positioning that using the ID of each LED to define every positioning unit cell. Therefore, the target can be traced more accurately than just using identity positioning technique. Unlike other VLC positioning systems, we use a solar cell panel as positioning Rx for the first time up to our knowledge; hence, the Rx field-of-view (FOV), detection area and the Rx sensitivity are significantly improved when compared with the PIN photodiode (PD). In addition, since solar cell is a passive Rx, it does not require power supply to operate; hence it does not only reducing the cost but also providing energy efficiency to the system. Energy harvesting and VLC signal detection could also be performed simultaneously using the solar cell Rx [11]. There are several application scenarios requiring relative high accuracy positioning. For example, the proposed work can be used for asset and people tracking. The optical Rxs can be equipped onto the wheelchairs in hospital for tracking the wheelchair movements. Besides, as solar cell can be physically flexible, it can be incorporated into wearable devices for patients in hospital or security guards in shopping mall for locations monitoring.

2. Proposed Architecture of Visible Light Positioning System

Fig. 1 shows the proposed architecture of the visible light positioning system. The whole space can be divided into several small positioning unit cells, which consist of three light sources. Each LED will transmit its ID signal by the format of on-off keying (OOK) with specific RF carrier frequency. The distribution of carriers is arranged as shown in Fig. 1. In the small unit cell, the detector will receive the signals from three LEDs simultaneously. Since the ID signals are modulated on three different carrier frequencies, the interference between each ID signal can be reduced. After demodulating the ID signals from three LEDs, the unit cell where the detector locates at can be known. As the detector move to another cell with different three LEDs, new ID signals will be detected, and therefore, the new unit cell can be determined. Because the distance from detector to each LED will change when it is moving in the unit cell, the received RF power of each ID signal will vary with the distance between detector to LED. Then, the trilateration positioning method is used to calculate the accurate position in the small unit cell. By

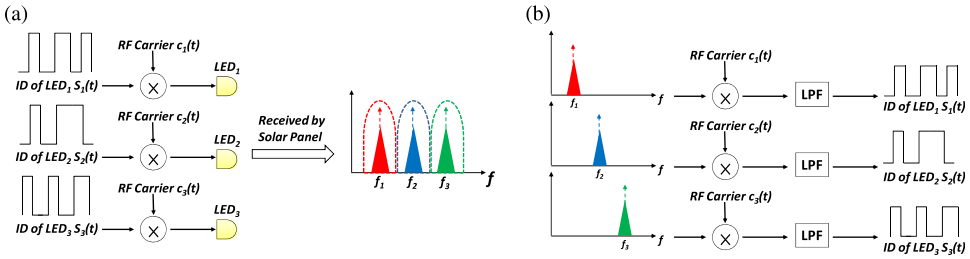

Fig. 2. Operation principle of ID transmission in small cell region. (a) Modulation of the transmitted signal. (b) Demodulation of the received signal.

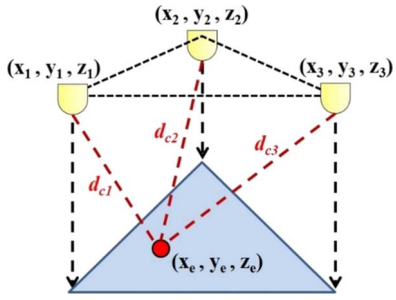

Fig. 3. Principle of the positioning method.

calculating continuously in the same way, the continuous and accurate indoor positioning by VLC can be achieved.

3. Operation Principle of Positioning

Fig. 2 presents the operation principle of ID signal transmission and the demodulation of the received signal in the position unit cell. First, three ID signals are up-converted to three different frequencies; that is, they are multiplied by three RF carrier signals, as shown in Fig. 2(a), and then they are transmitted to the corresponding LEDs. After received by the detector (solar cell panel is used here), three baseband signals modulated on the carriers can be filtered out respectively. For the demodulation, the filtered signals are multiplied again by the same corresponding carrier signals and then pass through different low-pass filters (LPFs). This can be implemented using digital signal processing (DSP). Thus, the ID signals of LEDs in the position unit cell can be demodulated as shown in Fig. 2(b). Here, the database of all position unit cells can be constructed with corresponding three identities of LEDs. As the ID signals are demodulated, the position at which unit cell can be known as well.

After obtaining the location at which unit cell, the trilateration positioning method is used to position more accurately in the small region of the cell. The principle of trilateration positioning method is to use three Txs sending RF signals with different frequencies to estimate the position of the Rx as shown in Fig. 3. Because the received signal powers at these three certain frequencies will change at different places, the distance from Rx to each Tx can be calculated according to the received signal power.

After obtaining the distances of the Rx from each Tx, the position of receiver can be estimated by solving

$$\begin{cases} (x_e - x_1)^2 + (y_e - y_1)^2 + (z_e - z_1)^2 = d_{c1}^2 \\ (x_e - x_2)^2 + (y_e - y_2)^2 + (z_e - z_2)^2 = d_{c2}^2 \\ (x_e - x_3)^2 + (y_e - y_3)^2 + (z_e - z_3)^2 = d_{c3}^2 \end{cases} \quad (1)$$

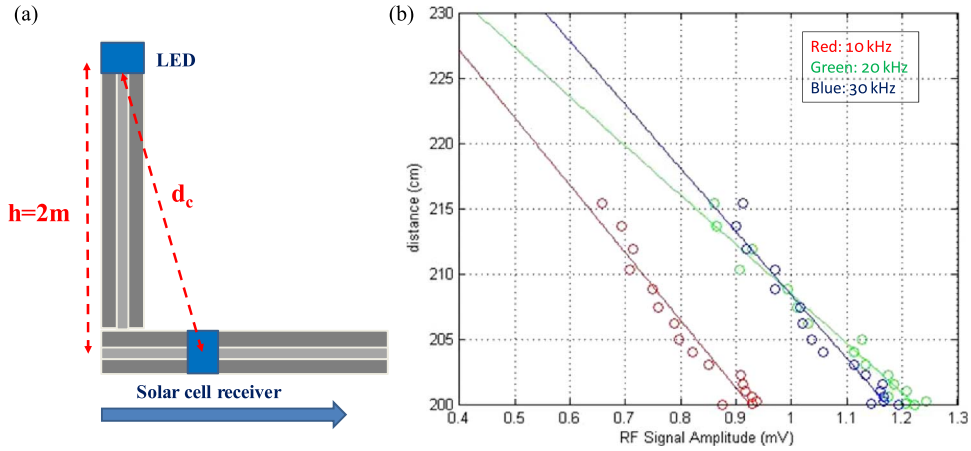

Fig. 4. (a) Setup to measure the relation of distance and RF signal power. (b) Measured results and the fitting curve.

where x_i, y_i, and z_i, $(i = 1, 2, 3)$ are the coordinates of three transmitters; and d_{c1}, d_{c2}, and d_{c3} are the line-of-sight distances as shown in Fig. 3. Here, we set z_e equals to zero for convenience because we only discuss two dimensional positioning in this work. Besides, we assume the height of each light on the ceiling is the same; that is, $z_1 = z_2 = z_3$. Then the estimated position (x_e, y_e) can be calculated using two linear equations, which can be simply obtained by subtracting the second and third equations from the first in (1), and the two linear equations in the condition of can be expressed in matrix form as $AX = B$, where A, X, and B are illustrated as

$$A = \begin{bmatrix} x_2 - x_1 & y_2 - y_1 \\ x_3 - x_1 & y_3 - y_1 \end{bmatrix}, X = \begin{bmatrix} x_e \\ y_e \end{bmatrix}, \text{ and } B = \begin{bmatrix} \frac{\left(d_{c1}^2 - d_{c2}^2 + x_2^2 + y_2^2 - x_1^2 - y_1^2\right)}{2} \\ \frac{\left(d_{c1}^2 - d_{c3}^2 + x_3^2 + y_3^2 - x_1^2 - y_1^2\right)}{2} \end{bmatrix}. \quad (2)$$

4. Experiment Setup

The VLC positioning system contains two experiments. First, the relationship of the LED-to-Rx distances and the RF signal powers is obtained. Here, the RF signals at different carrier frequencies are measured respectively to construct the relation curves. Second, the position of the Rx can be calculated by solving the equation as mentioned in last section based on the trilateration and using the relation curves obtained in the first experiment.

In the experiment, the LED chips used are from Cree XR-E, phosphor-based cool-white with correlated color temperature (CCT) of 5000 K. The electric current used to drive each LED chip is about 350 mA, and the typical lumen output is 100 lm. Each LED lamp is consists of six LED chips in cascade. Our proposed work is to provide positioning and lighting simultaneously. Since each of our LED lamp (light bulb) is consists of six LED chips; a diffuser is used to increase the lighting uniformity. The luminance half angle of each LED lamp is 30°. The diffuser introduces optical loss and the received optical power 2 m away from the LED lamp with the diffuser is only 300 lux. A bias-tee circuit is used to combined the RF signal from the arbitrary waveform generator and the 18 V direct-current (DC) from a power supply in each LED lamp. Fig. 4(a) shows the first experimental setup used to obtain the relation curves of the LED-to-Rx distances and the RF signal powers. The vertical distance h is fixed at 2 m, which represents the height between the ceiling LED lamp and the solar cell Rx. The solar cell used (SC-9728) is commercially available with $V_{op}/I_{op} = 6$ V/15 mA. It is fabricated based on amorphous silicon and with the dimension of $96.8 \times 28 \times 2$ mm. The model of typical solar cell used as VLC receiver and energy harvesting can be found in [12]. When the Rx moves horizontally from the origin, the signal

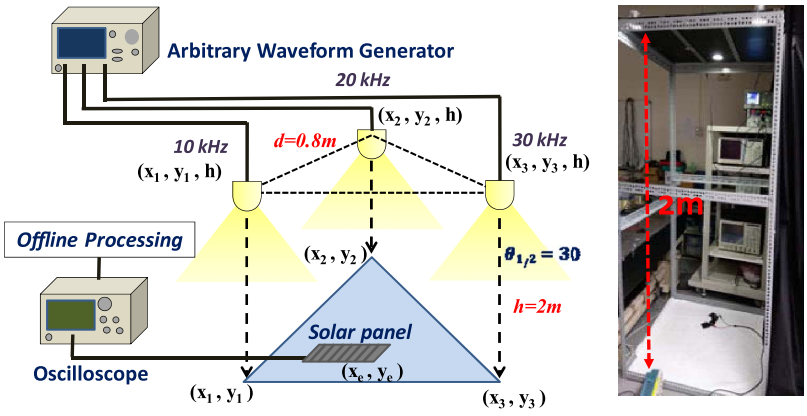

Fig. 5. Experiment setup of positioning system. (Inset) Experimental rack built for the experiment.

power will decrease gradually. The three different carrier frequencies used in this experiment are 10 kHz, 20 kHz, and 30 kHz, and the relation curves are shown in Fig. 4(b).

The second experiment setup about the positioning implementation is shown as Fig. 5. The distance between each LED in the ceiling is 80 cm and the height is 2 m, which are close to the condition in real application. The inset of Fig. 5 also shows the experimental test-bed built for the evaluation. Here, we set x and y coordinates of three LED lamp as (0, 0.6 cm), (0.5 cm, 80 cm), and (67.3 cm, 40 cm). The three electrical data signals with different carrier frequencies are first constructed using offline MATLAB program and generated via two arbitrary waveform generators (Tektronix AFG3252C and Agilent 33220A). These RF signals have frequencies of 10 kHz, 20 kHz, and 30 kHz. Solar panel is used as the passive optical Rx, which converts the received light signal into electrical signal. Here, the Rx will receive three different RF signals from different LED lamps in the unit cell simultaneously. Then an real-time oscilloscope (Tektronix TDS 2022B) connected to the solar panel is used to retrieve the signals for analysis. After this, the signal demultiplexing and the positioning are both implemented using offline MATLAB program. The fast Fourier transform (FFT) is used to convert the received signal into frequency spectrum. There will be three tones at 10 kHz, 20 kHz, and 30 kHz with different levels. Then we can use the relation curve measured before to deduce the location of the Rx.

5. Experiment Results and Discussion

Fig. 6(a)–(d) show the experimental spectra of received RF signals at several positions, such as (0, 0.6 cm), (0.5 cm, 80 cm), (67.5 cm, 40 cm), and (30 cm, 40 cm), respectively. At (0, 0.6 cm), (0.5 cm, 80 cm), and (67.5 cm, 40 cm), since these positions are exactly below the corresponding LEDs, the received RF signal tone is largest at frequencies of 10 kHz, 20 kHz and 30 kHz respectively. We record the amplitudes at these three frequencies and then use the relation curve in Fig. 4(b) to get the distance from Rx to each LED. After solving the equations in (1), the positioning result can be obtained. Fig. 6(e) illustrates the histogram of the positioning errors. More than 85% of the measurement results have position errors less than 10 cm. As the distance between the ceiling LED lamps and the Rx is 2 m, the received power at the Rx is only ~300 lux. The limited resolution is mainly caused by the low signal-to-noise ratio (SNR) of the received signal. In the test-bed, the distance between each LED in the ceiling is 80 cm and the height is 2 m. The received power of the Rx after 2 m transmission distance is only ~300 lux and the illuminance of a typical room should be 500 lux. The resolution could be improved by enhancing the illuminance of the LED lamps; or by decreasing the distance between the LED lamps in the ceiling.

Then, we analyze the ID signal transmission by using BER in the position unit cell. The modulation format of the ID signal is OOK and the data rate is 2 kbit/s. The low data rate is due to

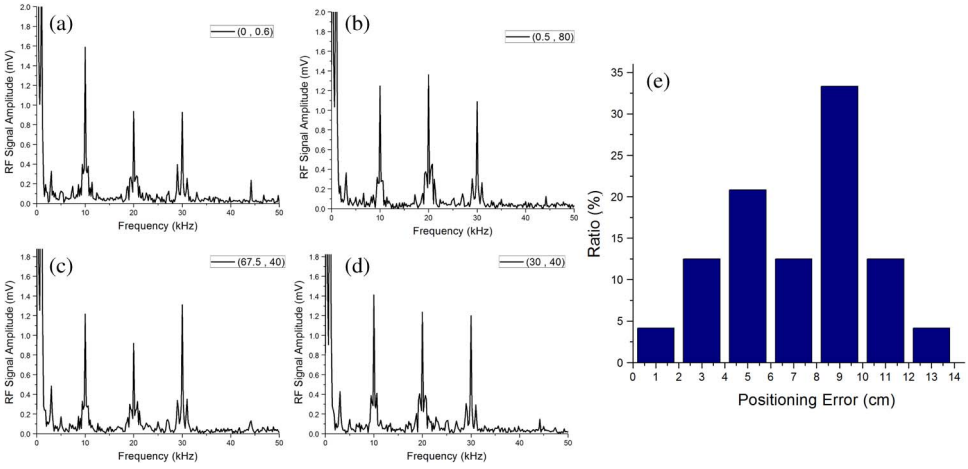

Fig. 6. Spectrum of the received signal (a) at (0, 0.6), (b) at (0.5, 80), (c) at (67.5, 40), and (d) at (30, 40). (e) Histogram of positioning error.

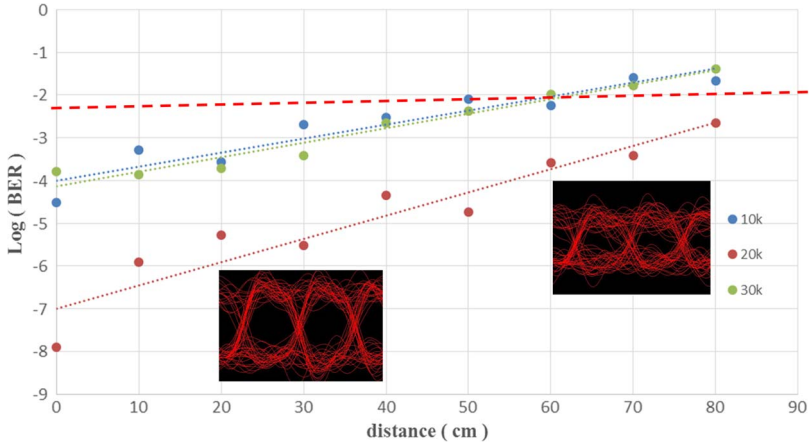

Fig. 7. BER performance of the ID signal transmission with carrier frequencies of 10 kHz, 20 kHz, and 30 kHz. (Inset) Eye diagrams of demodulated signal at carrier frequency of 20 kHz at 0-cm (directly below the LED) and 80-cm offsets.

limited bandwidth of the solar panel Rx. However, we believe that this data rate is enough for sending ID and navigation information. After receiving the signal at the solar cell panel, the scheme described in Fig. 2 is used to demodulate the ID signals. The measured BER results are shown in Fig. 7, the distances in x-axis represents the horizontal offsets of the Rx from the LED lamp. Therefore, 0 cm means the solar cell Rx is put directly below the LED. It can be seen that at most positions in the unit cell region, the BER can satisfy the 7% forward error correction (FEC) requirement of 3.8×10^{-3} (dotted line). The decrease in signal performance when offset disance increases is due to the reduce in SNR of the received signal. The insets of Fig. 7 show the demodulated eye-diagrams of signal with carrier frequency of 20 kHz at distance 0 cm and 80 cm respectively. A poorer eye-diagram is measured at 80 cm since the received optical power is very weak; but the FEC limit can still be achieved.

6. Conclusion

Unlike other VLC positioning systems, in this work, we proposed and experimentally demonstrated an indoor positioning system using solar-cell as a VLC Rx. The solar cell has much higher FOV, detection area and the Rx sensitivity when compared with the PIN PD. In addition, the

solar cell is a passive Rx, and it does not require power supply to operate. Energy harvesting and VLC signal detection can also be performed simultaneously. This system utilized a trilateration method combining with ID positioning to achieve a more accurate indoor positioning system than only using ID positioning technique. In the proof-of-concept experiment, the distance between each LED is 80 cm, and the height is 2 m, which can emulate the practical indoor situation. More than 85% of the measurement results have position errors less than 10 cm. For the ID signal transmission, the data rate is 2 kbit/s, and the BER at most of the positions in the unit cell can satisfy the FEC requirement. This technique could integrate with wearable device providing indoor positioning function with low cost.

References

[1] C. W. Chow, C. H. Yeh, Y. Liu, and Y. F. Liu, "Digital signal processing for light emitting diode based visible light communication," *IEEE Photon. Soc. Newslett.*, vol. 26, pp. 9–13, 2012.
[2] Y. C. Chi, D. H. Hsieh, C. T. Tsai, H. Y. Chen, H. C. Kuo, and G. R. Lin, "450-nm GaN laser diode enables high-speed visible light communication with 9-Gbps QAM-OFDM," *Opt. Exp.*, vol. 23, pp. 13051–13059, 2015.
[3] W. Y. Lin *et al.,* "10 m/500 Mbps WDM visible light communication systems," *Opt. Exp.*, vol. 20, pp. 9919–9924, 2012.
[4] C. H. Chang *et al.,* "A 100-Gb/s multiple-input multiple-output visible laser light communication system," *J. Lightw. Technol.*, vol. 32, pp. 4723–4729, 2014.
[5] Z. Wang, C. Yu, W. D. Zhong, J. Chen, and W. Chen, "Performance of a novel LED lamp arrangement to reduce SNR fluctuation for multi-user visible light communication systems," *Opt. Exp.*, vol. 20, pp. 4564–4573, 2012.
[6] S. Wu, H. Wang, and C. H. Youn, "Visible light communications for 5G wireless networking systems: From fixed to mobile communications," *IEEE Netw.*, vol. 28, no. 6, pp. 41–45, Nov./Dec. 2014.
[7] Y. U. Lee, S. Baang, J. Park, Z. Zhou, and M. Kavehrad, "Hybrid positioning with lighting LEDs and Zigbee multihop wireless network," in *Proc. SPIE Broadband Access Commun. Technol. VI*, 2012, vol. 8282, pp. 1–7.
[8] W. Zhang, M. I. S. Chowdhury, and M. Kavehrad, "Asynchronous indoor positioning system based on visible light communications," *Opt. Eng.*, vol. 53, no. 4, 2014, Art. no. 045105.
[9] M. Yasir, S. W. Ho, and B. N. Vellambi, "Indoor positioning system using visible light and accelerometer," *J. Lightw. Technol.*, vol. 32, pp. 3306–3316, 2014.
[10] Y. Liu, C. W. Hsu, H. Y. Chen, K. Liang, C. W. Chow, and C. H. Yeh, "Visible-light communication multiple-input multiple-output technology for indoor lighting, communication, and positioning," *Opt. Eng.*, vol. 54, no. 12, 2015, Art. no. 120502.
[11] Y. Liu, H. Y. Chen, K. Liang, C. W. Hsu, C. W. Chow, and C. H. Yeh, "Visible light communication using receivers of camera image sensor and solar cell," *IEEE Photon. J.*, vol. 8, no. 1, Feb. 2016, Art. no. 7800107.
[12] Z. Wang, D. Tsonev, S. Videv, and H. Haas, "On the design of a solar-panel receiver for optical wireless communications with simultaneous energy harvesting," *IEEE J. Sel. Areas Commun.*, vol. 33, no. 8, pp. 1612–1623, Aug. 2015.